Encapsulation of MEH-PPV:PCBM Hybrids in the Cores of Block Copolymer Micellar Assemblies: Photoinduced Electron Transfer in a Nanoscale Donor−Acceptor System

Suxiao Wang, James William Ryan Amita Singh, Jason Gerard Beirne, Emilio Palomares, and Gareth Redmond

†School of Chemistry, University College Dublin, Belfield, Dublin 4, Ireland

‡Institute of Chemical Research of Catalonia (ICIQ), Avinguda Països Catalans 16, 43007 Tarragona, Spain

§Institució Catalana de Recerca i Estudis Avancats, (ICREA), Passeig Lluís Companys 23, 08010 Barcelona, Spain

* Supporting Information

ABSTRACT: The objective of this work is to demonstrate that conjugated polymer:fullerene hybrid nanoparticles encapsulated in the hydrophobic cores of triblock copolymer micelles may successfully act as spatially confined donor−acceptor systems capable of facilitating photoinduced charge carrier separation. To this end, aqueous dispersions of poly[2-methoxy-5-(2-ethylhexyloxy)-1,4-phenylene-vinylene] (MEH-PPV) nanoparticles were first prepared by solubilization of the polymer in the cores of poly(oxyethylene)−poly(oxypropylene)−poly(oxyethylene) triblock copolymer, Pluronic F-127 micelles. A number of significant optical spectroscopic changes were observed on transfer of the conjugated polymer from a nonaqueous solvent to the aqueous micellar environment. These were primarily attributed to increased interchain interactions due to conjugated polymer chain collapse during encapsulation in the micellar cores.

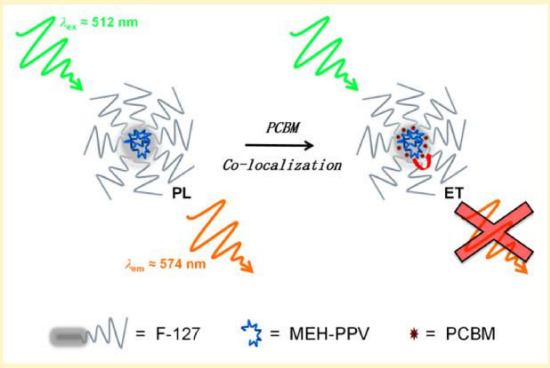

When prepared in buffer solution, the micelles exhibited good long-term collodial stability. When MEH-PPV micelles were blended by the addition of controlled amounts of [6,6]-phenyl-C_{61}-butyric acid methyl ester (PCBM), the observed correspondence of photoluminescence emission quenching, quantum yield decreases, and emission lifetime shortening with increasing PCBM concentration indicated efficient photoinduced donor-to-acceptor charge transfer between MEH-PPV and the fullerenes in the cores of the micelles, an assignment that was confirmed by transient absorption spectroscopic monitoring of carrier photogeneration and recombination.

INTRODUCTION

Hybrid materials that combine semiconducting conjugated polymers with either inorganic (nanoparticles or semiconductor quantum dots) or organic (polymers or small molecules) components as nanocomposites are important candidates for applications ranging from sensing to optoelectronics and energy conversion.[1−3] For example, nanocomposites based on conjugated polymers and colloidal quantum dots are key candidates for applications in bulk heterojunction solar cells, photodetectors, and light-emitting diodes.[4−6] With respect to the photovoltaics application, nanocomposites of conjugated polymers and the electron acceptor [6,6]-phenyl-C_{61}-butyric acid methyl ester (PCBM) have also shown significant promise.[7,8] Future development and optimization of these hybrid materials will require a deeper understanding of the critical processes, such as light absorption, energy transfer, and charge transfer, which occur in such systems.

One possible way to facilitate these studies may be to create model systems, composed of the relevant material building blocks arranged in a controlled manner, which are amenable to detailed experimental investigations. In this regard, there is significant current interest in studying nanoparticles of conjugated polymer-based nanocomposites because they present systems in a state intermediate between that of a small number of molecules and a bulk material.[9,10] As such, nanoparticles of these hybrid materials may offer the functionality that is available from bulk materials while providing reduced heterogeneity of properties as well as attractive strategies for the formation of active layers and heterojunctions in practical devices.[11,12] In this context, formation of composite nanoparticles of poly[2-methoxy-5-(2-ethylhexyloxy)-1,4-phenylenevinylene (MEH-PPV) or poly(3-hexylthiophene-2,5-diyl) (P3HT) with PCBM, by reprecipitation of the materials from a good solvent into water, followed by characterization of their structural and photophysical properties, along with demonstration of photoinduced charge

transfer, has already been reported.[13,14] Further, preliminary applications of such nanoparticles to fabrication of bulk heterojunction photovoltaic devices have also been reported.[15,16]

An alternative synthetic approach to the controlled formation of nanoparticles of nanocomposites is to exploit the tendency of amphiphilic block copolymers to self-assemble into nano-sized micelles, the interiors of which may be used to spatially localize or encapsulate selected molecules, polymers, or particles.[17,18] For example, diblock copolymer micelles have been employed as tools for the rational control of energy transfer processes involving metallic nanoparticles and dye molecules by spatial engineering of donor and acceptor locations and separations.[19,20] Importantly, the use of block copolymer micelles as hosts for emissive conjugated polymers, with exciting applications to fluorescence-based cellular imaging and biosensing, has also recently been reported.[21, 22] In addition, the self-assembly of micellar aggregates has been successfully used a vehicle for the encapsulation and controlled positioning of both semiconductor quantum dots and full-erenes, respectively.[23,24] At the next level of structural complexity, co-organization of both conjugated polymers and quantum dots has been achieved using the amphiphilic block copolymer assembly approach, with preliminary evidence of electronic energy transfer interactions being presented, while the incorporation of micellar assemblies consisting of conjugated diblock copolymers linked with PCBM derivatives[25,26] into prototype photovoltaic devices has also been reported.

In this paper, we report on the preparation of stable aqueous dispersions of conjugated polymer nanoparticles based on the well-known polymer MEH-PPV and the characterization of the structural and photophysical properties of these particles both in the pure form and when blended by addition of known amounts of PCBM. To this end, MEH-PPV nanoparticles were prepared using a micellization approach by solubilization of the conjugated polymer in the hydrophobic cores of triblock copolymer micelles based on the commercial surfactant Pluronic F-127 (hereinafter referred to as F-127). This amphiphilic triblock copolymer consists of poly(ethylene oxide) (PEO) and poly(propylene oxide) (PPO) blocks with a PEO−PPO−PEO structure.[27] F-127 exhibits complex phase behavior with the potential to self-assemble into polymeric micelles with various morphologies depending on solvent quality, polymer concentration, and solution temperature.[28] We find that although MEH-PPV is completely insoluble in water, the polymer can be dispersed in aqueous micellar media formed using F-127. The resulting homogeneous dispersions, with no observable precipitation, suggested that the emissive, hydro-phobic conjugated polymer material was successfully encapsu-lated within the hydrophobic interiors of the self-assembled F-127 nanostructures. This approach permitted detailed assess-ment of the photophysical properties of the micelle-encapsulated MEH-PPV chains in the absence and presence of added PCBM molecules.

EXPERIMENTAL METHODS

Materials. Poly[2-methoxy-5-(2-ethylhexyloxy)-1,4-phenylene-vinylene] (MEH-PPV) with a weight-average molecular weight of 250 000 g/mol was purchased from American Dye Source, Inc. [6,6]-Phenyl-C_{61}-butyric acid methyl ester (PCBM), with a molecular weight of 910.88 g/mol, was purchased from Solenne B.V., Groningen, The Netherlands. Pluronic F-127 ($M_w \approx 12\,600$), chloroform (spectrophotometric grade, ≥99.8%), phosphate buffered saline (PBS) tablets, and tetrahydrofuran (CHROMASOLV for HPLC, 99.9%) were purchased from Sigma-Aldrich, Inc. Deionized water (>16.1 MΩ·cm, Milli-Q, SMillipore Corp.) was used for all aqueous solutions.

Preparation of Micelles. Micelles were formulated using a modified literature process.[29] MEH-PPV solution was prepared by dissolving it into chloroform in a sealed glass bottle while heating to 60 °C and stirring vigorously for 2 h. The solution was allowed to cool to room temperature with stirring overnight. The resulting solution was transparent. An appropriate volume of this solution, containing 10 μg of MEH-PPV, was mixed with 30 mg of F-127 in 400 μL of chloroform. The chloroform was evaporated to dryness by N_2 gas flow. Deionized water (1 mL) or PBS buffer solution (0.1 M, pH 7.4; 1 mL) was added to the vial, and this was shaken vigorously for 3 min using a vortex stirrer to create an aqueous dispersion of self-assembled MEH-PPV micelles with a concentration of 30.01 mg/mL. To prepare PCBM-doped micelles, 10 mg PCBM was first dissolved into 100 mL of chloroform under stirring for 1 h to make a PCBM solution with a concentration of 0.1 mg/mL. PCBM micelles were synthesized by dissolving 30 mg of F-127, 10 μg of MEH-PPV, and different amounts of PCBM (3, 6, 9, 12, 15, and 25 wt % PCBM or ca. 0.8, 1.7, 2.5, 3.3, 4.1, and 6.9 × 10^3 mol % PCBM, respectively) in 400 μL of chloroform. The chloroform was evaporated to dryness by N_2 gas flow. Deionized water (1 mL) was added to the vial, and this was shaken vigorously for 3 min using a vortex stirrer to create an aqueous dispersion of self-assembled MEH-PPV:PCBM nanomicelles.

Physical Characterization. Dynamic light scattering (DLS) and zeta-potential measurements were carried using a Zetasizer Nano ZS system (Malvern Instuments, Ltd., UK). DTS Application 5.10 software was employed to analyze the data obtained. Transmission electron microscopy (TEM) images of MEH-PPV micelles were acquired using a FEI Tecnai G2 20 Twin microscope (FEI, Inc.). Samples were prepared by dropping 20 μL of micelle suspension onto Formvar-coated copper grids, waiting for 1 min, and wicking away excess liquid using filter paper (1001-125; Whatman, Inc.). Each grid was gently rinsed once with deionized water and left to air-dry.

Optical Spectroscopy. To minimize artifacts, such as optical scattering, scattering, saturation, or reabsorption, dilute samples (<0.1 AU) were used to measure absorption and photoluminescence spectra. UV−vis absorption spectra were acquired using a double-beam spectrophotometer (V-650; Jasco, Inc.). Water or solvent was used as a reference. Photoluminescence spectra were acquired using a QuantaMasterTM 40, (PTI, Inc.), equipped with a pulsed Xe short arc discharge lamp and Czerny-Turner monochromators. Photolumines-cence quantum yields were determined by using the same fluorometer equipped with an integrating sphere (Labsphere, Inc.). A black light illuminator (Gel Logic 200; Kodak, Ltd.) was used when recording true-color emission photographs (Lumix DMC-TZ30; Panasonic, Corp.) Transient absorption measurements were undertaken using a home-built system: a nitrogen laser (GL-3300; PTI, Inc.) coupled with a dye laser (GL-301; PTI, Inc.), equipped with Coumarin 102 dye, provided pump excitation at 460 nm. A 150 W tungsten lamp (PTI, Inc.) was used as the probe source. Input pulses (1 Hz) were provided by a function generator (TG330; Thurlby Thandar Instruments, Ltd.). The optical signal was detected using a silicon diode-based system which was connected to a module for signal filtering and amplification (Costronics Electronics, Ltd.). Signal acquisition was managed by a digital oscilloscope (TDS 2022; Tektronix, Inc.). Fluorescence lifetimes were measured by time-correlated single photon counting using an FS900 CDT spectrometer (Edinburgh Instruments, Ltd.) and a liquid nitrogen cryostat (Oxford Instruments, Lts.) connected to an ITC-2 controller. Samples were excited at 470 nm using a picosecond pulsed diode laser source. The data acquired from this instrument were fitted using analysis software (Fluofit, 4.6; PicoQuant, GmbH). For both types of transient measurements, all samples were rigorously deaerated prior to data collection.

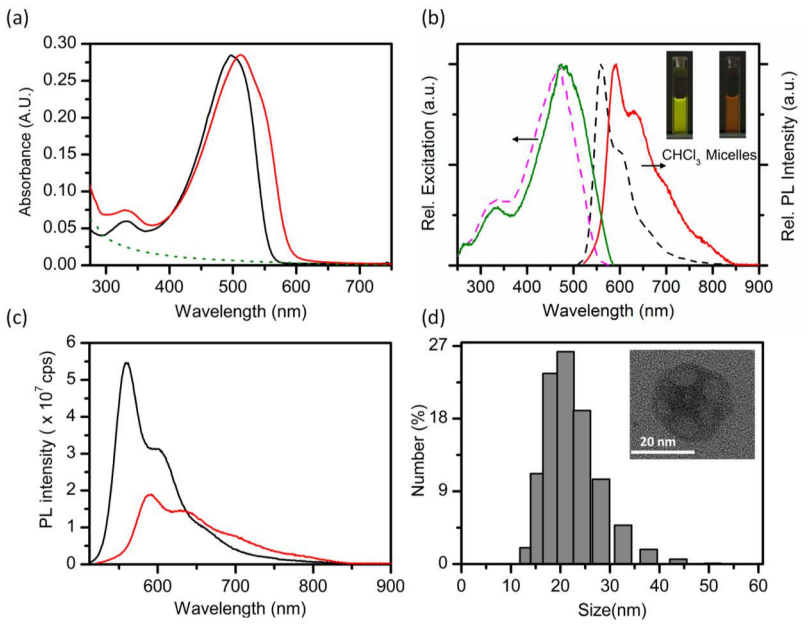

Figure 1. (a) Absorption spectra of an MEH-PPV solution in chloroform (black line) and of the corresponding conjugated polymer nanomicelles prepared in water (red line). The dashed green line is an absorption spectrum of empty F-127 micelles. (b) Intensity-normalized excitation and emission spectra of a MEH-PPV solution (dashed lines) and of MEH-PPV micelles (solid lines). Insets: photographs of MEH-PPV emission from a chloroform solution and a micellar suspension under black light illumination. (c) Emission spectra of MEH-PPV in chloroform solution (black line) and in aqueous nanomicellar suspension (red line). (d) Number-average hydrodynamic size distribution of MEH-PPV micelles. Inset: transmission electron micrographs of a typical MEH-PPV micelle.

RESULTS AND DISCUSSION

MEH-PPV and PCBM in Micellar Media. MEH-PPV chains were dispersed in micellar media by exposing the polymer to water in the presence of F-127 triblock copolymer surfactant. The resulting aqueous dispersions were stable and clear (not turbid) and presented a characteristic pink color associated with light absorption by the conjugated polymer. Typical absorption spectra measured for a solution of MEH-PPV in chloroform (black line), an aqueous dispersion of MEH-PPV with F-127 (red line), and an aqueous dispersion of F-127 (green dashed line) are shown in Figure 1a. The MEH-PPV/chloroform solution spectrum exhibited an absorption maximum at 498 nm ascribed to intrachain $\pi-\pi^*$ transitions along with a shoulder at ca. 560 nm assigned to optical absorption by aggregate species.[30−34] This absorption maximum was significantly red-shifted, to 512 nm, and slightly broadened in the presence of F-127 in water. Corresponding photoluminescence excitation spectra and emission spectra measured for MEH-PPV in organic solvent solution and in aqueous dispersion with F-127, respectively, are shown in Figure 1b. The observed excitation spectral changes were consistent with those noted above for the absorption spectra. The MEH-PPV/chloroform solution emission spectrum exhibited a characteristic vibronic progression with peaks located at ca. 560, 600, and 660 nm arising from the $S_1 \rightarrow S_0$ 0−0 singlet electronic transition of MEH-PPV with 0−1 and 0−2 vibronic replicas and with a possible small contribution due to emission by aggregate species at wavelengths near the 0−2 emission band.[31,35,36] In contrast, the emission spectrum measured for MEH-PPV in the presence of F-127 in water exhibited a significant spectral red-shift (e.g., 0−0 emission band shifted to ca. 592 nm) and peak broadening along with an increase in the relative peak intensities at the red end of the emission spectrum. Reflecting these spectral changes, both chloroform solutions and aqueous dispersions exhibited fluorescence emission with distinctly different, characteristic colors under black light illumination (see Figure 1b, inset).

These spectral changes were attributed to increased interchain interactions due to conjugated polymer chain collapse during encapsulation into hydrophobic F-127 micellar cores, resulting in a change in the polarizability of the environment around each polymer chain segment and in the formation of a fraction of red-shifted aggregate species with energetic disorder.[13,35−37] In the latter circumstances, following photoexcitation, multistep energy transfer would be expected to cause a red- shift of the photoluminescence spectrum as compared to that of the polymer in a good solvent, and this phenomenon has been often observed, for example, following formation of thin films.[38] In concert with this observed red-shift in emission, a pronounced decrease in photoluminescence quantum yield (PL QY) was measured following formation of the MEH-PPV micelles (chloroform solution PL QY: 0.27; micelle dispersion PLQY: 0.15) (see Figure 1c). This observation was also consistent with polymer chain aggregation in the condensed phase.

Dynamic light scattering (DLS) methods were employed to measure the hydrodynamic size distributions of the F-127-solubilized MEH-PPV dispersions in water. The measured data indicated a z-average particle diameter (d_z) for the micelles of 61 nm (polydispersity index, PDI: 0.3) and a number-average particle diameter (d_n) of 21 nm (see Figure 1d). For reference, a number-average particle diameter of 21 nm was also obtained for F-127-only micelles (see Figure S1, Supporting Informa-tion). A representative transmission electron microscopy (TEM) image of a MEH-PPV micelle is shown in Figure 1d, inset. The zeta potentials of the micelles were also measured and were found to be approximately 0 mV, with a conductivity of ca. 3 mS/cm, in all cases (see Figure S2a). Therefore, the aqueous solubilization of the MEH-PPV by F-127, giving rise to

aggregation of conjugated polymer chains, was demonstrated to be feasible.

To provide additional benchmark information, PCBM micelles were prepared by exposing the molecules to water in the presence of F-127 surfactant. The resulting aqueous dispersions were stable and clear (not turbid). The spectroscopic properties PCBM in organic solvent of solution and in aqueous medium were measured and compared. Typical absorption spectra measured for a solution of PCBM in chloroform (black line), an aqueous dispersion of PCBM with F-127 (red line), and an aqueous dispersion of F-127 (green dashed line) are shown in Figure 2a. The PCBM solution

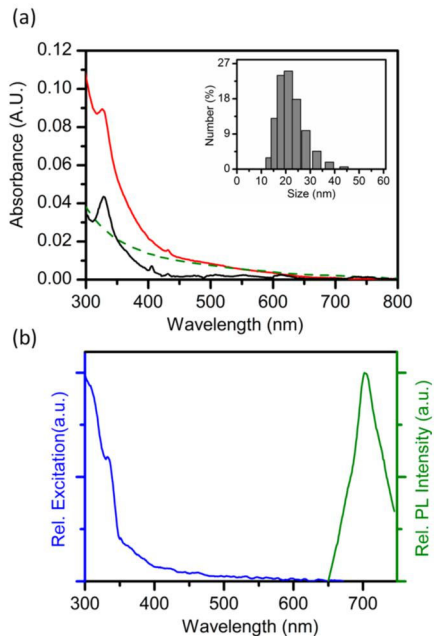

Figure 2. (a) Absorption spectra of PCBM solution in chloroform (black line) and of the corresponding PCBM nanomicelles prepared in water (red line). The dashed green line is an absorption spectrum of empty F-127 micelles. Inset: number-average hydrodynamic size distribution of PCBM micelles. (b) Intensity-normalized excitation and emission spectra of the PCBM micelles.

spectrum exhibited optical absorption mainly in the near-UV region with only weak absorption in the visible region (absorption peak at 326 nm with a weak tail extending toward the red). These observations are consistent with reported solution optical absorption spectra of the parent molecule, C_{60}, and reflect the fact that the high symmetry of the C_{60} molecule causes transitions in the visible region to be symmetry-forbidden while higher energy transitions are fully allowed.[39−41] In contrast, the absorption spectrum measured for an aqueous dispersion of PCBM with F-127 exhibited greater absorption in the visible region (350−700 nm), with an absorption peak at 329 nm, consistent with observations made for thin films of PCBM.[42,43] An apparent weak absorption tail that extended as far as 800 nm was not thought to be due to light scattering or other measurement artifacts; such spectral features have previously been reported for C_{60} thin films.[44,45] In addition, photoluminescence excitation and emission spectra measured for PCBM in aqueous dispersion with F-127 are shown in Figure 2b. The emission spectrum exhibited a band with maximum at ca. 700 nm which has previously been assigned to emission from the S_1 singlet excited state of C_{60}.[46] The corresponding excitation spectrum closely resembled the measured absorption spectrum. Overall, the previous studies, cited above, which described the contrasting optical properties of isolated fullerene molecules in solution with fullerene films, assigned the increased light absorption exhibited by fullerene films in the visible region to the presence of intermolecular charge transfer (CT) transitions. This suggested that the increased optical absorption observed herein for aqueous dispersions of PCBM with F-127 can be assigned, by analogy, to increased intermolecular interactions that occur between aggregated PCBM molecules following their encapsulation into hydrophobic F-127 micellar cores, consequently resulting in a measurable CT absorption.

Dynamic light scattering methods were employed to measure the hydrodynamic size distributions of the F-127-solubilized PCBM dispersions in water. The measured data indicated a z-average particle diameter, d_z, of 29 nm (PDI: 0.05) and a number-average particle diameter, d_n, of 22 nm (see Figure 2a, inset). The zeta potentials of the micelles were also measured and were found to be approximately 0 mV, in all cases (see Figure S2b).

MEH-PPV:PCBM Hybrids in Micellar Media. To explore the feasibility of hybrid MEH-PPV:PCBM nanostructures, MEH-PPV and PCBM were exposed to water in the presence of F-127 surfactant. The spectroscopic properties of MEH-PPV:PCBM hybrids (25 wt % PCBM) in aqueous micellar medium were then measured and directly compared with MEH-PPV micelles. Typical absorption spectra measured for MEH-PPV-only (black line) and MEH-PPV:PCBM (red line) aqueous micellar dispersions are shown in Figure 3a. Both spectra exhibited the characteristic absorption profiles associated with micellar MEH-PPV while, in addition, the MEH-PPV:PCBM absorption spectrum exhibited obvious additional optical absorbance at wavelengths below 400 nm due to PCBM.

Hydrodynamic size distribution data were measured for the F-127-solubilized MEH-PPV:PCBM (25 wt %) dispersions in water and indicated a z-average particle diameter, d_z, of 40 nm (PDI: 0.3) and a number-average particle diameter, d_n, of 21 nm (see Figure 3b). The zeta potentials of the micelles were also measured and were found to be approximately 0 mV, in all cases (see Figure S2c). Some representative TEM images of the micelles are shown in Figure 3c−e. The typical size was ca. 40 nm, similar to the z-average particle size. Importantly, pinpoint-like regions of high contrast (dark clusters in the image) were observed in all images of PCBM-doped micelles, consistent with sequestration/aggregation of water insoluble PCBM molecules as a PCBM-rich phase in the hydrophobic cores of the F-127 micelles.

The colloidal stability of the micelles in a range of environments was also studied. As determined by DLS measurements, MEH-PPV:PCBM (25 wt %) micelles showed a clear size stability with a number-average hydrodynamic diameter of 21 nm, over the pH range 2.0−12.0 in water (see Figure 4). Likewise, the zeta potentials measured for the micelles appeared to be stable, at approximately 0 mV, at each pH value (see Figure 4). These data indicated that medium pH did not affect the micelles; i.e., apparently, no degradation or aggregation occurred under these condition, consistent with observations reported for empty F-127 micelles.[47,48] The stability of the MEH-PPV:PCBM (25 wt %) micelles was also studied as a function of storage duration (see Figure S2d). The dispersions appeared to be quite stable, with no significant

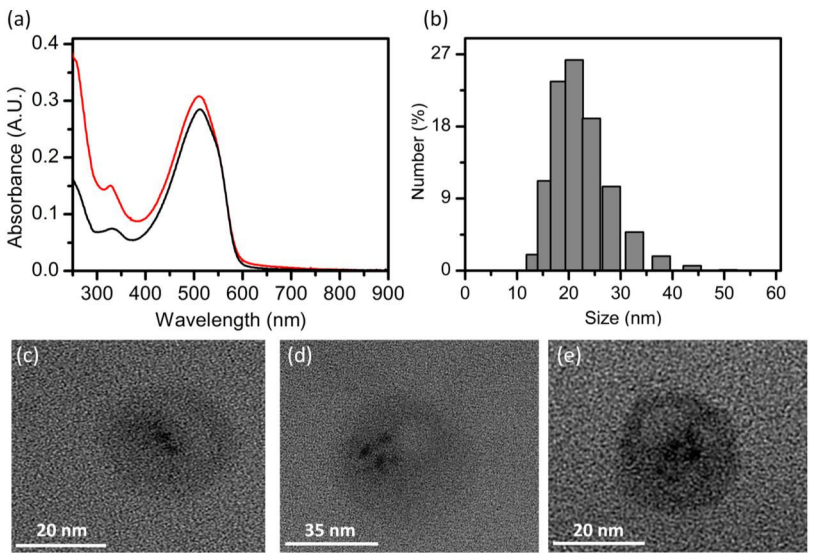

Figure 3. (a) Absorption spectra of MEH-PPV micelles (black line) and MEH-PPV:PCBM (25 wt %) micelles (red line) prepared in water. (b) Number-average hydrodynamic size distribution data measured for the MEH-PPV:PCBM (25 wt %) micelles in water. (c−e) Transmission electron micrographs typical MEH-PPV:PCBM (25 wt %) micelles.

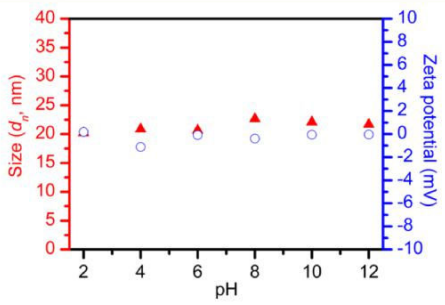

Figure 4. Number-average hydrodynamic size (red triangles) and zeta potential (empty blue circles) values measured for aqueous MEH-PPV:PCBM (25 wt %) micelles over the pH range 2.0−12.0.

observable time-dependent changes in hydrodynamic diameter, when micelles were stored as dispersions in PBS buffer solutions over 7 days.[49]

MEH-PPV:PCBM Micellar Hybrids: Varying PCBM Concentration. In order to better understand the properties of these novel hybrid MEH-PPV:PCBM nanostructures, a range of MEH-PPV:PCBM micelles that were doped with progressively greater amounts of added PCBM (0−25 wt %) were prepared in water. Photoluminescence spectra measured for aqueous MEH-PPV:PCBM micelles as a function of the amount of added PCBM (0−25 wt %) are shown in Figure 5a. A decrease in emission intensity was found to occur with increasing PCBM concentration with emission quenching of approximately 21, 26, 31, 34, 42, and 68% being observed at added PCBM concentrations of 3, 6, 9, 12, 15, and 25 wt %, respectively. A similar systematic trend was observed during measurements of photoluminescence quantum yield data for aqueous MEH-PPV nanomicelles as a function of the amount of added PCBM (0−25 wt %) (see Figure 5b). Specifically, the measured fluorescence quantum yields were found to take values of 0.15, 0.13, 0.11, 0.10, 0.09, 0.08, and 0.04 at added PCBM concentrations of 0, 3, 6, 9, 12, 15, and 25 wt %, respectively. Importantly, dynamic light scattering measure-ments carried out on these hybrid micelles indicated a clear size stability with a number-average hydrodynamic diameter of 22

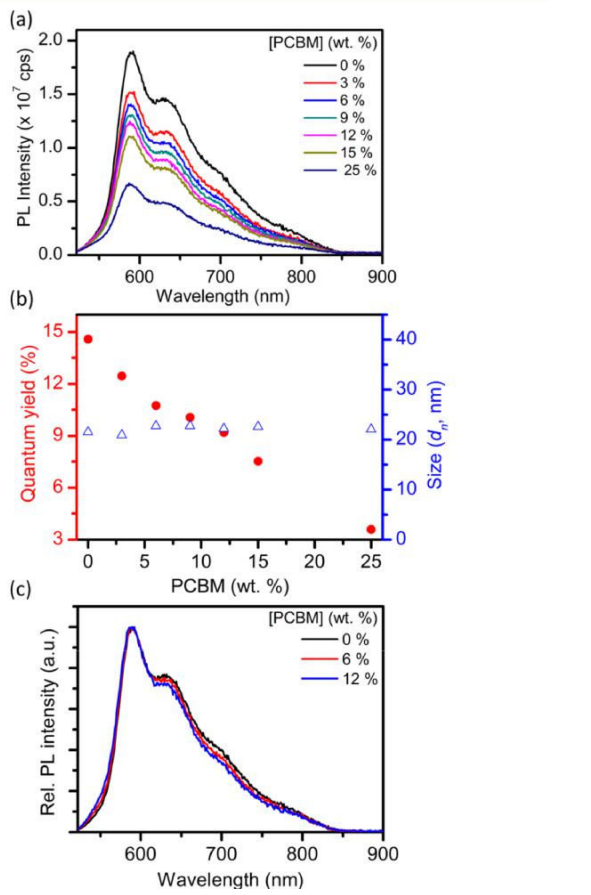

Figure 5. (a) Photoluminescence emission spectra measured for aqueous MEH-PPV:PCBM nanomicelles as a function of the amount of added PCBM (0−25 wt %). (b) Photoluminescence quantum yields measured for aqueous MEH-PPV:PCBM nanomicelles as a function of the amount of added PCBM (0−25 wt %) (red dots) and number-average hydrodynamic sizes of aqueous MEH-PPV:PCBM micelles as a function of the amount of added PCBM (0−25 wt %) (blue triangles).(c) Intensity-normalized emission spectra overlaid to show spectral changes that arise with increasing PCBM concentrations.

nm being observed over the dopant concentration range (see Figure 5b).

Photoluminescence decay data were also measured using the time-correlated single photon counting technique (see Figure 6a). Excited state lifetimes were extracted from the decay traces

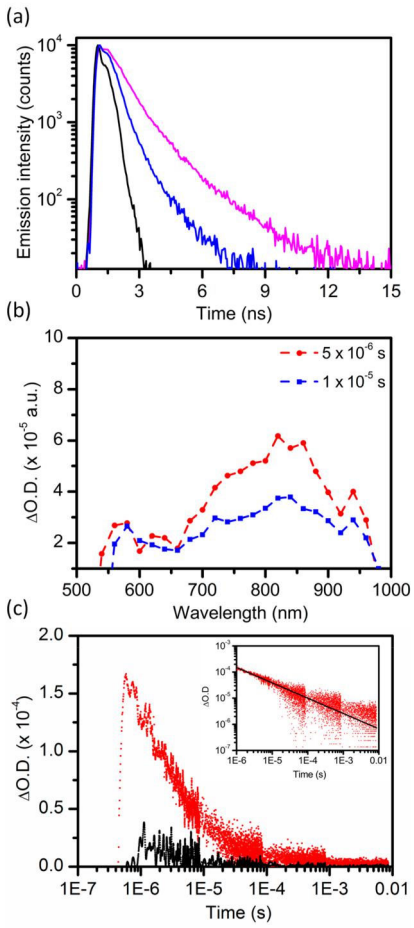

Figure 6. (a) Photoluminescence decays measured for MEH-PPV micelles (pink line) and MEH-PPV:PCBM micelles (15 wt %; blue line) prepared in water; instrument response function (black line). (b) Transient absorption spectra recorded at 5 and 10 μs after 460 nm pulsed excitation of aqueous MEH-PPV:PCBM (15 wt %) micelles. (c) Transient absorption decays recorded at 840 nm after 460 nm pulsed excitation of aqueous MEH-PPV micelles (black line) and MEH-PPV:PCBM (15 wt %) micelles (red line), respectively. Inset: power law fitting of the transient decay measured for the MEH-PPV:PCBM (15 wt %) micelle.

using commercial software by fitting the measured photoluminescence decay traces with double-exponential functions. Photoluminescence lifetimes were estimated by weight-averaging the decay components. The weight-averaged photoluminescence lifetime estimated for aqueous MEH-PPV micelles was 0.83 ns while the photoluminescence lifetime estimated for aqueous MEH- PPV:PCBM (15 wt %) micelles was observed to decrease to 0.35 ns, further illustrating the effect of added PCBM on the photophysical properties of the conjugated polymer. The photoluminescence radiative (k_r) and nonradiative (k_{nr}) rate constants were estimated by combining the quantum yield (ϕ), where $\phi = k_r/(k_r + k_{nr})$, and fluorescence lifetime (τ) data, where $\tau = (k_r + k_{nr})^{-1}$, specifically, by using the formulas $k_r = \phi/\tau$ and $k_{nr} = 1/(\tau -$ k_r). Values for the radiative and nonradiative rate constants estimated in this manner for aqueous MEH-PPV micelles were 1.8×10^8 s^{-1} and 3.7×10^8 s^{-1}, respectively, while the corresponding values estimated for aqueous MEH-PPV:PCBM (15 wt %) micelles were 2.1×10^8 s^{-1} and 2.7×10^9 s^{-1}, respectively.

The observed correspondence of photoluminescence emis-sion quenching, quantum yield decreases, emission lifetime shortening, and increased nonradiative rate with increasing PCBM concentration was attributed to nonradiative quenching of MEH-PPV excited states by photoinduced electron transfer from MEH-PPV donors to PCBM acceptors colocalized in the hydrophobic cores of the F-127 micelles. In this regard, e□cient photoinduced donor-to-acceptor charge transfer between MEH-PPV and fullerenes in thin films has also been previously studied in detail and formed the basis for early bulk heterojunction organic photovoltaic devices, with quenching of donor conjugated polymer fluorescence being a strong indicator of such a process.[50−55] However, energy transfer quenching may constitute an alternative, competing pathway for nonradiative decay of the MEH-PPV excited states. While Förster energy transfer is expected to be negligible in this system, given the small overlap between the PCBM absorption and MEH-PPV emission spectra, PCBM and MEH-PPV molecules may well be in close enough contact to facilitate Dexter energy transfer. In this regard, since the electrons that would be expected to be present in the charge-separated states have been detected during electron spin resonance measure-ments, it appears that although polymer-to-PCBM energy transfer is potentially a competing mechanism, charge transfer is the dominant relaxation pathway.[56,57]

A further indication of the colocalization of MEH-PPV and PCBM molecules within the hydrophobic interiors of the F-127 micelles may be found by considering subtle changes that arise in the photoluminescence emission spectrum of micellar MEH-PPV as a function of added PCBM (see Figure 5c). With increasing PCBM concentration, the MEH-PPV emission spectrum is slightly blue-shifted (by 4 nm), and the vibronic structure is changed. The former changes were previously reported during studies of aqueous MEH-PPV: PCBM nanoparticles prepared by a reprecipitation process and were attributed to a reduction in MEH-PPV chain conjugation length due to steric effects caused by the presence of PCBM that resulted in polymer chain conformations with increased kinking and bending of the backbones.[13] In addition, the presence of PCBM was thought to reduce interchain π-stacking interactions thereby limiting exciton transport due to compartmentalization of the polymer chains, preventing excitons from reaching low-energy sites. The latter changes in vibronic structure are consistent with the changing aggregation state of the conjugated polymer chains as interchain interactions diminish with increasing PCBM concentrations, a decreasing intensity of the 0−1 vibronic peak relative to the 0−0 peak occurs.[13]

Finally, the dynamics of charge carrier photogeneration and recombination in aqueous MEH-PPV:PCBM micelles was explored using transient absorption spectroscopic methods.[58,59] Transient absorption spectra recorded at 5 and 10 μs after pulsed 460 nm excitation of aqueous MEH-PPV:PCBM (15 wt %) micelles are shown in Figure 6b. A broad photoinduced transient absorption that extended from 530 to 970 nm was observed. The maximum difference in optical density (OD) was centered at approximately 840 nm. This spectral feature,

which was in good agreement with transient spectroscopic data previously reported for PPV/acceptor systems, was assigned to optical absorption by hole polarons trapped on the MEH-PPV chains following rapid (at time scales below that of the measurement system temporal resolution) photoinduced electron transfer from MEH-PPV to the PCBM electron acceptors.[56,60−62]

The decay dynamics of the transient absorption signal were measured at 840 nm for both MEH-PPV micelles and MEH-PPV:PCBM (15 wt %) micelles in water (see Figure 6c). The magnitude of the polaron signal observed for MEH-PPV micelles was significantly smaller than that observed for MEH-PPV:PCBM micelles, consistent with very low charge photo-generation in the undoped micelles in the absence of electron acceptors. For the MEH-PPV:PCBM micelles, two phases of recombination dynamics were evident: a fast phase from 500 ns to10 μs and a slow phase from 10 μs into the ms time regime. This biphasic behavior was very similar to that reported previously for MDMO-PPV:PCBM blend films.[63] The fast phase was assigned to recombination of free polarons that were generated when the density of photogenerated polarons exceeded the density of localized states.[64] The slow phase was fit to a power law decay ($OD \propto t^{-\alpha}$ where OD is the change in optical density, t is time, and $\alpha = T/T_0$ where T is the temperature and T_0 is characteristic temperature of the distribution of charge traps; here, $\alpha = 0.59$) and was assigned to bimolecular recombination of dissociated polarons in the presence of an exponential tail of intra-band-gap localized (trapped) states (see Figure 6c, inset).[59] The extracted value of α was higher than that observed for MDMO-PPV:PCBM blend films (α = 0.4; where MDMO-PPV denotes poly[2-methoxy-5-(3′,7′-dimethyloctyloxy)-1,4-phenylenevinylene]), indicative of a relatively low level of deep traps for the MEH-PPV:PCBM micelles.[59,63,65] Very similar behavior has previously been reported for a variety of other conjugated polymer:PCBM films based on, e.g., poly(3-hexylthiophene) and other polythio-phenes and, most recently, a number of novel MEH-PPV oligomers and a related copolymer.[66−72] In addition, Durrant and co-workers have shown that the exponent (α) in such power-law decays is dependent upon the polymer film morphology and the film processing conditions, with values of α ranging between 0.3 and 0.7 being attributed to variations in trap density.[70,71] Overall, this transient spectroscopic data provided strong confirmation of the nonradiative quenching of MEH-PPV excited states by photoinduced electron transfer from MEH-PPV donors to PCBM acceptors colocalized in the hydrophobic cores of the F-127 micelles.

CONCLUSION

In this work, aqueous dispersions of conjugated polymer nanoparticles based on MEH-PPV were prepared by solubilization of the polymer in the hydrophobic cores of F-127 micelles. Absorption and photoluminescence excitation and emission spectral changes were observed on transfer of the conjugated polymer from a nonaqueous solvent to an aqueous micellar environment and were attributed to increased interchain interactions due to conjugated polymer chain collapse during encapsulation in the hydrophobic micellar cores. When prepared in buffer solution, the micelles exhibited good long-term collodial stability. When the MEH-PPV micelles were blended by the addition of controlled amounts of PCBM, the observed correspondence of photoluminescence emission quenching, quantum yield decreases, and emission lifetime shortening with increasing PCBM concentration indicated efficient photoinduced donor-to-acceptor charge transfer between MEH-PPV and the fullerenes in the cores of the micelles. This assignment was subsequently confirmed by transient absorption spectroscopic measurements that demonstrated that the MEH-PPV:PCBM micelles acted as spatially confined donor−acceptor systems capable of successfully facilitating photoinduced charge carrier separation.

ASSOCIATED CONTENT

* Supporting Information

The Supporting Information is available free of charge on the ACS Publications website at DOI: 10.1021/acs.langmuir.5b04053.

Data sets presenting zeta potential distributions measured for micelles and hydrodynamic size stability over time (PDF)

AUTHOR INFORMATION

Corresponding Author

*Tel + 353 1 716 2881; e-mail gareth.redmond@ucd.ie (G.R.).

Present Addresses

J.W.R.: International Centre for Young Scientists, Global Research Center for Environment and Energy based on Nanomaterials Science (GREEN), National Institute for Materials Science (NIMS), 1-1 Namiki, Tsukuba, Ibaraki 305-0044, Japan.

A.S.: The University of Texas at Austin, McKetta Department of Chemical Engineering, 200 E Dean Keeton St. Stop, C0400, Austin, TX 78712-1589.

Notes

The authors declare no competing financial interest.

ABBREVIATIONS

PCBM, [6,6]-phenyl-C_{61}-butyric acid methyl ester; MEH-PPV, poly[2-methoxy-5-(2-ethylhexyloxy)-1,4 phenylenevinylene]; MDMO-PPV, poly[2-methoxy-5-(3′,7′-dimethyloctyloxy)-1,4-phenylenevinylene]; P3HT, poly(3-hexylthiophene-2,5-diyl); F-127, Pluronic F-127; PEO, poly(ethylene oxide); PPO, poly(propylene oxide); M_w, molecular weight; PBS, phosphate buffered saline; DLS, dynamic light scattering; AU, absorbance units; au, arbitrary units; UV−vis, ultraviolet−visible; TEM, transmission electron microscopy; PL QY, photoluminescence quantum yield; CT, charge transfer.

REFERENCES

(1) Holder, E.; Tessler, N.; Rogach, A. L. Hybrid Nanocomposite Materials with Organic and Inorganic Components for Opto-Electronic Devices. J. Mater. Chem. 2008, 18, 1064−1078.

(2) Talapin, D. V.; Lee, J.-S.; Kovalenko, M. V.; Shevchenko, E. V. Prospects of Colloidal Nanocrystals for Electronic and Optoelectronic Applications. Chem. Rev. 2010, 110, 389−458.

(3) Reiss, P.; Couderc, E.; De Girolamo, J.; Pron, A. Conjugated Polymers/Semiconductor Nanocrystals Hybrid Materials Preparation, Electrical Transport Properties and Applications. Nanoscale 2011, 3, 446−489.

(4) Colvin, V.; Schlamp, M.; Alivisatos, A. Light-Emitting Diodes Made from Cadmium Selenide Nanocrystals and a Semiconducting Polymer. Nature 1994, 370, 354−357.

(5) An, T. K.; Park, C. E.; Chung, D. S. Polymer−Nanocrystal Hybrid Photodetectors with Planar Heterojunctions Designed Strategically to Yield a High Photoconductive Gain. Appl. Phys. Lett. 2013, 102, 193306.

(6) de Freitas, J. N.; Grova, I. R.; Akcelrud, L. C.; Arici, E.; Sariciftci, N. S.; Nogueira, A. F. The Effects of Cdse Incorporation into Bulk Heterojunction Solar Cells. J. Mater. Chem. 2010, 20, 4845−4853.
(7) Hoppe, H.; Niggemann, M.; Winder, C.; Kraut, J.; Hiesgen, R.; Hinsch, A.; Meissner, D.; Sariciftci, N. S. Nanoscale Morphology of Conjugated Polymer/Fullerene - Based Bulk - Heterojunction Solar Cells. Adv. Funct. Mater. 2004, 14, 1005−1011.
(8) He, X.; Gao, F.; Tu, G.; Hasko, D. G.; Hüttner, S.; Greenham, N. C.; Steiner, U.; Friend, R. H.; Huck, W. T. Formation of Well - Ordered Heterojunctions in Polymer: Pcbm Photovoltaic Devices. Adv. Funct. Mater. 2011, 21, 139−146.
(9) Wu, C.; Szymanski, C.; McNeill, J. Preparation and Encapsulation of Highly Fluorescent Conjugated Polymer Nanoparticles. Langmuir 2006, 22, 2956−2960.
(10) Wu, C.; Bull, B.; Szymanski, C.; Christensen, K.; McNeill, J. Multicolor Conjugated Polymer Dots for Biological Fluorescence Imaging. ACS Nano 2008, 2, 2415−2423.
(11) Labastide, J. A.; Baghgar, M.; Dujovne, I.; Yang, Y.; Dinsmore, A. D.; G. Sumpter, B.; Venkataraman, D.; Barnes, M. D. Polymer Nanoparticle Superlattices for Organic Photovoltaic Applications. J. Phys. Chem. Lett. 2011, 2, 3085−3091.
(12) Bag, M.; Gehan, T. S.; Renna, L. A.; Algaier, D. D.; Lahti, P. M.; Venkataraman, D. Fabrication Conditions for Efficient Organic Photovoltaic Cells from Aqueous Dispersions of Nanoparticles. RSC Adv. 2014, 4, 45325−45331.
(13) Tenery, D.; Worden, J. G.; Hu, Z.; Gesquiere, A. J. Single Particle Spectroscopy on Composite MEH-PPV/PCBM Nano-particles. J. Lumin. 2009, 129, 423−429.
(14) Tenery, D.; Gesquiere, A. J. Interplay between Fluorescence and Morphology in Composite MEH-PPV/PCBM Nanoparticles Studied at the Single Particle Level. Chem. Phys. 2009, 365, 138−143.
(15) Darwis, D.; Holmes, N.; Elkington, D.; Kilcoyne, A. D.; Bryant, G.; Zhou, X.; Dastoor, P.; Belcher, W. Surfactant-Free Nanoparticulate Organic Photovoltaics. Sol. Energy Mater. Sol. Cells 2014, 121, 99−107.
(16) Gehan, T. S.; Bag, M.; Renna, L. A.; Shen, X.; Algaier, D. D.; Lahti, P. M.; Russell, T. P.; Venkataraman, D. Multiscale Active Layer Morphologies for Organic Photovoltaics through Self-Assembly of Nanospheres. Nano Lett. 2014, 14, 5238−5243.
(17) Liu, R.; Wang, S.; Yao, J.; Xu, W.; Li, H. Cross-Linked Reverse Micelles with Embedded Water Pools: A Novel Catalytic System Based on Amphiphilic Block Copolymers. RSC Adv. 2014, 4, 38234− 38240.
(18) Hu, J.; Wu, T.; Zhang, G.; Liu, S. Efficient Synthesis of Single Gold Nanoparticle Hybrid Amphiphilic Triblock Copolymers and Their Controlled Self-Assembly. J. Am. Chem. Soc. 2012, 134, 7624− 7627.
(19) Izmodenova, S.; Kislov, D.; Kucherenko, M. Accelerated Nonradiative Electron-Excitation Energy Transfer between Molecules in Aqueous Pools of Reverse Micelles Containing Encapsulated Silver Nanoparticles. Colloid J. 2014, 76, 683−693.
(20) Kim, K.-S.; Kim, J.-H.; Kim, H.; Laquai, F.; Arifin, E.; Lee, J.-K.; Yoo, S. I.; Sohn, B.-H. Switching Off Fret in the Hybrid Assemblies of Diblock Copolymer Micelles, Quantum Dots, and Dyes by Plasmonic Nanoparticles. ACS Nano 2012, 6, 5051−5059.
(21) Jung, Y.; Hickey, R. J.; Park, S.-J. Encapsulating Light-Emitting Polymers in Block Copolymer Micelles. Langmuir 2010, 26, 7540− 7543.
(22) Park, S.-J.; Kang, S.-G.; Fryd, M.; Saven, J. G.; Park, S.-J. Highly Tunable Photoluminescent Properties of Amphiphilic Conjugated Block Copolymers. J. Am. Chem. Soc. 2010, 132, 9931−9933.
(23) Zhang, M.; Wang, M.; He, S.; Qian, J.; Saffari, A.; Lee, A.; Kumar, S.; Hassan, Y.; Guenther, A.; Scholes, G. Sphere-to-Wormlike Network Transition of Block Copolymer Micelles Containing Cdse Quantum Dots in the Corona. Macromolecules 2010, 43, 5066−5074.
(24) Wang, X.-S.; Metanawin, T.; Zheng, X.-Y.; Wang, P.-Y.; Ali, M.; Vernon, D. Structure-Defined C_{60}/Polymer Colloids Supramolecular Nanocomposites in Water. Langmuir 2008, 24, 9230−9232.
(25) Wang, M.; Zhang, M.; Li, J.; Kumar, S.; Walker, G. C.; Scholes, G. D.; Winnik, M. A. Self-Assembly of Colloidal Quantum Dots on the Scaffold of Triblock Copolymer Micelles. ACS Appl. Mater. Interfaces 2010, 2, 3160−3169.
(26) Zhang, M.; Rene-Boisneuf, L.; Hu, Y.; Moozeh, K.; Hassan, Y.; Scholes, G.; Winnik, M. A. Preparation and Photo/Chemical-Activation of Wormlike Network Micelles of Core−Shell Quantum Dots and Block Copolymer Hybrids. J. Mater. Chem. 2011, 21, 9692− 9701.
(27) Schmolka, I. R. Artificial Skin I. Preparation and Properties of Pluronic F - 127 Gels for Treatment of Burns. J. Biomed. Mater. Res. 1972, 6, 571−582.
(28) Yu, G.-E.; Deng, Y.; Dalton, S.; Wang, Q.-G.; Attwood, D.; Price, C.; Booth, C. Micellisation and Gelation of Triblock Copoly (Oxyethylene/Oxypropylene/Oxyethylene), F127. J. Chem. Soc., Faraday Trans. 1992, 88, 2537−2544.
(29) Lim, C. K.; Lee, Y. D.; Na, J.; Oh, J. M.; Her, S.; Kim, K.; Choi, K.; Kim, S.; Kwon, I. C. Chemiluminescence - Generating Nanoreactor Formulation for near - Infrared Imaging of Hydrogen Peroxide and Glucose Level in Vivo. Adv. Funct. Mater. 2010, 20, 2644−2648.
(30) Hagting, J. G.; Vorenkamp, E. J.; Schouten, A. J. In-Plane Orientation in Langmuir-Blodgett Multilayers of a Partly Converted Flexible Poly(P-Phenylenevinylene)Precursor Polymer. Macromole-cules 1999, 32, 6619.
(31) Zheng, M.; Bai, F.; Zhu, D. Photophysical Process of Meh-Ppv Solution. J. Photochem. Photobiol., A 1998, 116, 143−145.
(32) Liu, Y.; Li, Q.; Xu, Y.; Jiang, X.; Zhu, D. Light-Emitting Diodes Based on High Electron Affinity Polymer Langmuir-Blodgett Films. Synth. Met. 1997, 85, 1279−1280.
(33) Traiphol, R.; Sanguansat, P.; Srikhirin, T.; Kerdcharoen, T.; Osotchan, T. Spectroscopic Study of Photophysical Change in Collapsed Coils of Conjugated Polymers: Effects of Solvent and Temperature. Macromolecules 2006, 39, 1165−1172.
(34) Traiphol, R.; Charoenthai, N.; Srikhirin, T.; Kerdcharoen, T.; Osotchan, T.; Maturos, T. Chain Organization and Photophysics of Conjugated Polymer in Poor Solvents: Aggregates, Agglomerates and Collapsed Coils. Polymer 2007, 48, 813−826.
(35) Nguyen, T.-Q.; Martini, I. B.; Liu, J.; Schwartz, B. J. Controlling Interchain Interactions in Conjugated Polymers: The Effects of Chain Morphology on Exciton-Exciton Annihilation and Aggregation in MHE-PPV Films. J. Phys. Chem. B 2000, 104, 237−255.
(36) Nguyen, T.-Q.; Doan, V.; Schwartz, B. J. Conjugated Polymer Aggregates in Solution: Control of Interchain Interactions. J. Chem. Phys. 1999, 110, 4068−4078.
(37) Tan, H.; Zhang, Y.; Wang, M.; Zhang, Z.; Zhang, X.; Yong, A. M.; Wong, S. Y.; Chang, A. Y.-c.; Chen, Z.-K.; Li, X. Silica-Shell Cross-Linked Micelles Encapsulating Fluorescent Conjugated Polymers for Targeted Cellular Imaging. Biomaterials 2012, 33, 237−246.
(38) Szymanski, C.; Wu, C.; Hooper, J.; Salazar, M. A.; Perdomo, A.; Dukes, A.; McNeill, J. Single Molecule Nanoparticles of the Conjugated Polymer MEH-PPV, Preparation and Characterization by near-Field Scanning Optical Microscopy. J. Phys. Chem. B 2005, 109, 8543−8546.
(39) Cook, S.; Ohkita, H.; Kim, Y.; Benson-Smith, J. J.; Bradley, D. D.; Durrant, J. R. A Photophysical Study of Pcbm Thin Films. Chem. Phys. Lett. 2007, 445, 276−280.
(40) Leach, S.; Vervloet, M.; Despres, A.; Breheret, E.; Hare, J. P.; Dennis, T. J.; Kroto, H. W.; Taylor, R.; Walton, D. R. Electronic Spectra and Transitions of the Fullerene C_{60}. Chem. Phys. 1992, 160, 451−466.
(41) Muccini, M. Optical Properties of Solid C_{60}. Synth. Met. 1996, 83, 213−219.
(42) Liu, Y.-X.; Summers, M. A.; Scully, S. R.; McGehee, M. D. Resonance Energy Transfer from Organic Chromophores to Fullerene Molecules. J. Appl. Phys. 2006, 99, 93521−93521.
(43) Savenije, T. J.; Kroeze, J. E.; Wienk, M. M.; Kroon, J. M.; Warman, J. M. Mobility and Decay Kinetics of Charge Carriers in Photoexcited PCBM/PPV Blends. Phys. Rev. B: Condens. Matter Mater. Phys. 2004, 69, 155205.
(44) Bensasson, R. V.; Bienvenüe, E.; Janot, J. M.; Land, E. J.; Leach, S.; Leboulaire, V.; Rassat, A.; Roux, S.; Seta, P. Photophysical

Properties of Three Methanofullerene Derivatives. Chem. - Eur. J. 1998, 4, 270−278.
(45) Katz, E.; Faiman, D.; Mishori, B.; Shapira, Y.; Isakina, A.; Strzhemechny, M. Disorder/Order Phase Transition in C60 Thin Films Studied by Surface Photovoltage Spectroscopy. J. Appl. Phys. 2003, 94, 7173−7177.
(46) Cook, S.; Ohkita, H.; Durrant, J. R.; Kim, Y.; Benson-Smith, J. J.; Nelson, J.; Bradley, D. D. Singlet Exciton Transfer and Fullerene Triplet Formation in Polymer-Fullerene Blend Films. Appl. Phys. Lett. 2006, 89, 101128.
(47) Chiappetta, D. A.; Sosnik, A. Poly (Ethylene Oxide)−Poly (Propylene Oxide) Block Copolymer Micelles as Drug Delivery Agents: Improved Hydrosolubility, Stability and Bioavailability of Drugs. Eur. J. Pharm. Biopharm. 2007, 66, 303−317.
(48) Determan, M. D.; Cox, J. P.; Seifert, S.; Thiyagarajan, P.; Mallapragada, S. K. Synthesis and Characterization of Temperature and Ph-Responsive Pentablock Copolymers. Polymer 2005, 46, 6933− 6946.
(49) Xiong, X.; Tam, K.; Gan, L. Hydrolytic Degradation of Pluronic F127/Poly (Lactic Acid) Block Copolymer Nanoparticles. Macro-molecules 2004, 37, 3425−3430.
(50) Deibel, C.; Dyakonov, V. Polymer−Fullerene Bulk Hetero-junction Solar Cells. Rep. Prog. Phys. 2010, 73, 096401.
(51) Chen, M.; Li, M.; Wang, H.; Qu, S.; Zhao, X.; Xie, L.; Yang, S. Side-Chain Substitution of Poly (3-Hexylthiophene)(P_3HT) by Pcbm Via Postpolymerization: An Intramolecular Hybrid of Donor and Acceptor. Polym. Chem. 2013, 4, 550−557.
(52) Morita, S.; Zakhidov, A. A.; Yoshino, K. Doping Effect of Buckminsterfullerene in Conducting Polymer: Change of Absorption Spectrum and Quenching of Luminescene. Solid State Commun. 1992, 82, 249−252.
(53) Kraabel, B.; Hummelen, J. C.; Vacar, D.; Moses, D.; Sariciftci, N.; Heeger, A.; Wudl, F. Subpicosecond Photoinduced Electron Transfer from Conjugated Polymers to Functionalized Fullerenes. J. Chem. Phys. 1996, 104, 4267−4273.
(54) Moses, D.; Dogariu, A.; Heeger, A. J. Ultrafast Detection of Charged Photocarriers in Conjugated Polymers. Phys. Rev. B: Condens. Matter Mater. Phys. 2000, 61, 9373.
(55) Meskers, S.; van Hal, P.; Spiering, A.; Hummelen, J.; van der Meer, A.; Janssen, R. Time-Resolved Infrared-Absorption Study of Photoinduced Charge Transfer in a Polythiophene-Methanofullerene Composite Film. Phys. Rev. B: Condens. Matter Mater. Phys. 2000, 61, 9917.
(56) Sariciftci, N.; Smilowitz, L.; Heeger, A. J.; Wudl, F. Photoinduced Electron Transfer from a Conducting Polymer to Buckminsterfullerene. Science 1992, 258, 1474−1476.
(57) Dyakonov, V.; Zoriniants, G.; Scharber, M.; Brabec, C.; Janssen, R.; Hummelen, J.; Sariciftci, N. Photoinduced Charge Carriers in Conjugated Polymer−Fullerene Composites Studied with Light-Induced Electron-Spin Resonance. Phys. Rev. B: Condens. Matter Mater. Phys. 1999, 59, 8019.
(58) Shuttle, C.; O'Regan, B.; Ballantyne, A.; Nelson, J.; Bradley, D.; De Mello, J.; Durrant, J. Experimental Determination of the Rate Law for Charge Carrier Decay in a Polythiophene: Fullerene Solar Cell. Appl. Phys. Lett. 2008, 92, 3311.
(59) Nelson, J. Diffusion-Limited Recombination in Polymer-Fullerene Blends and Its Influence on Photocurrent Collection. Phys. Rev. B: Condens. Matter Mater. Phys. 2003, 67, 155209.
(60) Kraabel, B.; McBranch, D.; Sariciftci, N.; Moses, D.; Heeger, A. Ultrafast Spectroscopic Studies of Photoinduced Electron Transfer from Semiconducting Polymers to C_{60}. Phys. Rev. B: Condens. Matter Mater. Phys. 1994, 50, 18543.
(61) van Hal, P. A.; Christiaans, M. P.; Wienk, M. M.; Kroon, J. M.; Janssen, R. A. Photoinduced Electron Transfer from Conjugated Polymers to Tio_2. J. Phys. Chem. B 1999, 103, 4352−4359.
(62) Smilowitz, L.; Sariciftci, N.; Wu, R.; Gettinger, C.; Heeger, A.; Wudl, F. Photoexcitation Spectroscopy of Conducting-Polymer−C_{60} Composites: Photoinduced Electron Transfer. Phys. Rev. B: Condens. Matter Mater. Phys. 1993, 47, 13835.
(63) Nogueira, A. F.; Montanari, I.; Nelson, J.; Durrant, J. R.; Winder, C.; Sariciftci, N. S.; Brabec, C. Charge Recombination in Conjugated Polymer/Fullerene Blended Films Studied by Transient Absorption Spectroscopy. J. Phys. Chem. B 2003, 107, 1567−1573.
(64) Clarke, T.; Ballantyne, A.; Jamieson, F.; Brabec, C.; Nelson, J.; Durrant, J. Transient Absorption Spectroscopy of Charge Photo-generation Yields and Lifetimes in a Low Bandgap Polymer/Fullerene Film. Chem. Commun. 2008, 89.
(65) Montanari, I.; Nogueira, A. F.; Nelson, J.; Durrant, J. R.; Winder, C.; Loi, M. A.; Sariciftci, N. S.; Brabec, C. Transient Optical Studies of Charge Recombination Dynamics in a Polymer/Fullerene Composite at Room Temperature. Appl. Phys. Lett. 2002, 81, 3001− 3003.
(66) Guo, J.; Ohkita, H.; Yokoya, S.; Benten, H.; Ito, S. Bimodal Polarons and Hole Transport in Poly (3-Hexylthiophene): Fullerene Blend Films. J. Am. Chem. Soc. 2010, 132, 9631−9637.
(67) Guo, J.; Ohkita, H.; Benten, H.; Ito, S. Charge Generation and Recombination Dynamics in Poly (3-Hexylthiophene)/Fullerene Blend Films with Different Regioregularities and Morphologies. J. Am. Chem. Soc. 2010, 132, 6154−6164.
(68) Clarke, T. M.; Jamieson, F. C.; Durrant, J. R. Transient Absorption Studies of Bimolecular Recombination Dynamics in Polythiophene/Fullerene Blend Films. J. Phys. Chem. C 2009, 113, 20934−20941.
(69) Shuttle, C. G.; O'Regan, B.; Ballantyne, A. M.; Nelson, J.; Bradley, D. D.; Durrant, J. R. Bimolecular Recombination Losses in Polythiophene: Fullerene Solar Cells. Phys. Rev. B: Condens. Matter Mater. Phys. 2008, 78, 113201.
(70) Ohkita, H.; Cook, S.; Astuti, Y.; Duffy, W.; Tierney, S.; Zhang, W.; Heeney, M.; McCulloch, I.; Nelson, J.; Bradley, D. D. Charge Carrier Formation in Polythiophene/Fullerene Blend Films Studied by Transient Absorption Spectroscopy. J. Am. Chem. Soc. 2008, 130, 3030−3042.
(71) Kim, Y.; Cook, S.; Tuladhar, S. M.; Choulis, S. A.; Nelson, J.; Durrant, J. R.; Bradley, D. D.; Giles, M.; McCulloch, I.; Ha, C.-S. A Strong Regioregularity Effect in Self-Organizing Conjugated Polymer Films and High-Efficiency Polythiophene: Fullerene Solar Cells. Nat. Mater. 2006, 5, 197−203.
(72) Tan, T. A.; Clarke, T. M.; James, D.; Durrant, J. R.; White, J. M.; Ghiggino, K. P. Synthesis and Photo-Induced Charge Separation of Confined Conjugation Length Phenylene Vinylene-Based Polymers. Polym. Chem. 2013, 4, 5305−5309.